3

# Hydrogeology of the Poitou Threshold

T. Gaillard and M. Moreau

## Aquifers of the Poitou threshold

### *Two main aquifers*

The sedimentary cover of the Poitou Threshold (Branger et al., 2026) consists of Lower and Middle Jurassic deposits. Consequently, only two aquifers were historically defined by the first geologists who studied the region's hydrogeology (Welsch, 1912). These are referred to as the Supra-Toarcian Aquifer and the Infra-Toarcian Aquifer, named after the intervening Toarcian marls that separate them (Welsch, 1912). Continuous coring from boreholes drilled at the Hydrogeological Experimental Site of Poitiers University (HES) has provided a detailed lithostratigraphic and hydrogeological description of the Jurassic sequence (Fig. 1).

Beneath the site, the granitic basement occurs at a depth of 158 m. The Infra-Toarcian Aquifer overlies this basement and is approximately 21 m thick. Its basal section comprises clays and dolomites of Hettangian–Sinemurian age (150–158 m), overlain by bioclastic marly limestones of Pliensbachian age (135–150 m). This aquifer is overlain by the Toarcian marls, which are about 15 m thick (120–135 m).


DOI: https://doi.org/10.1051/978-2-7598-3934-6.c003

Above the Toarcian marls lies the Supra-Toarcian Aquifer. Its base consists of marly limestones passing upward into more carbonate-rich and oolitic facies of Aalenian age (101–120 m). The overlying Bajocian limestones (46–101 m) display a range of facies, from bioclastic to gravelly textures, and include a distinct interval of white oolites between 80 and 83 m. This unit is followed by fine-gravelly limestones interbedded with flint of Bathonian age (21–46 m) and capped by "chalky" white limestones of Callovian age (6–21 m). Near the surface, these limestones are weathered to form a red clay horizon (0–6 m).

The Infra-Toarcian Aquifer is confined, whereas the Supra-Toarcian Aquifer is unconfined. The substantial thickness of the Toarcian marls ensures effective hydraulic separation between the two, except in faulted zones where vertical displacements exceed 20 m.

## *Piezometric map*

At the HES, groundwater levels in the Infra-Toarcian Aquifer range from 95 to 100 m NGF (meters above sea level, French elevation datum), while those in the Supra-Toarcian Aquifer range from 100 to 105 m NGF. The piezometry of the Supra-Toarcian Aquifer is relatively well documented as a result of several monitoring campaigns carried out between the Vienne River (east of Poitiers) and the Clain River (Coirier et al., 1968).

In 2004, two additional piezometric surveys were conducted on the Supra-Toarcian Aquifer. Each survey covered approximately 800 measurement points (Marchais and Bichot, 2005). The piezometric map derived from the October 2004 survey is considered representative of low-water conditions (Fig. 2).

The main drainage axis in the Clain River basin trends south–north from Vivonne to Poitiers. The downcutting by the Clain began during interglacial stages of the Mindel and Riss glaciations. Secondary drainage axes, oriented perpendicular to the main one, correspond to younger valleys incised during the Weichselian: the Clouère River (Gencay–Vivonne axis), the Vonne River west of Vivonne, the Auxance River north of Poitiers, and the Boivre River. In these valleys, Supra-Toarcian limestones are deeply eroded, and riverbeds may locally cut down to the Infra-Toarcian Aquifer. Piezometric gradients in the area range between 0.5% and 1%.

The piezometric watershed of the Clain differs markedly from its topographic watershed (Fig. 3). To the east, a north–south-oriented groundwater divide separates the Vienne and Clain basins. This divide is near the axis of the Miosson River, which is perched and hydraulically disconnected from the Supra-Toarcian Aquifer in its upstream reaches. The piezometric divide defines the hydrogeological catchments of the Vienne and Clain, which do not coincide with their surface watershed boundaries. The piezometric catchment of the Clain is smaller than its topographic watershed due to a westward offset of the divide. As early as 1968, Coirier et al. attributed this offset to the lower base level of the Vienne

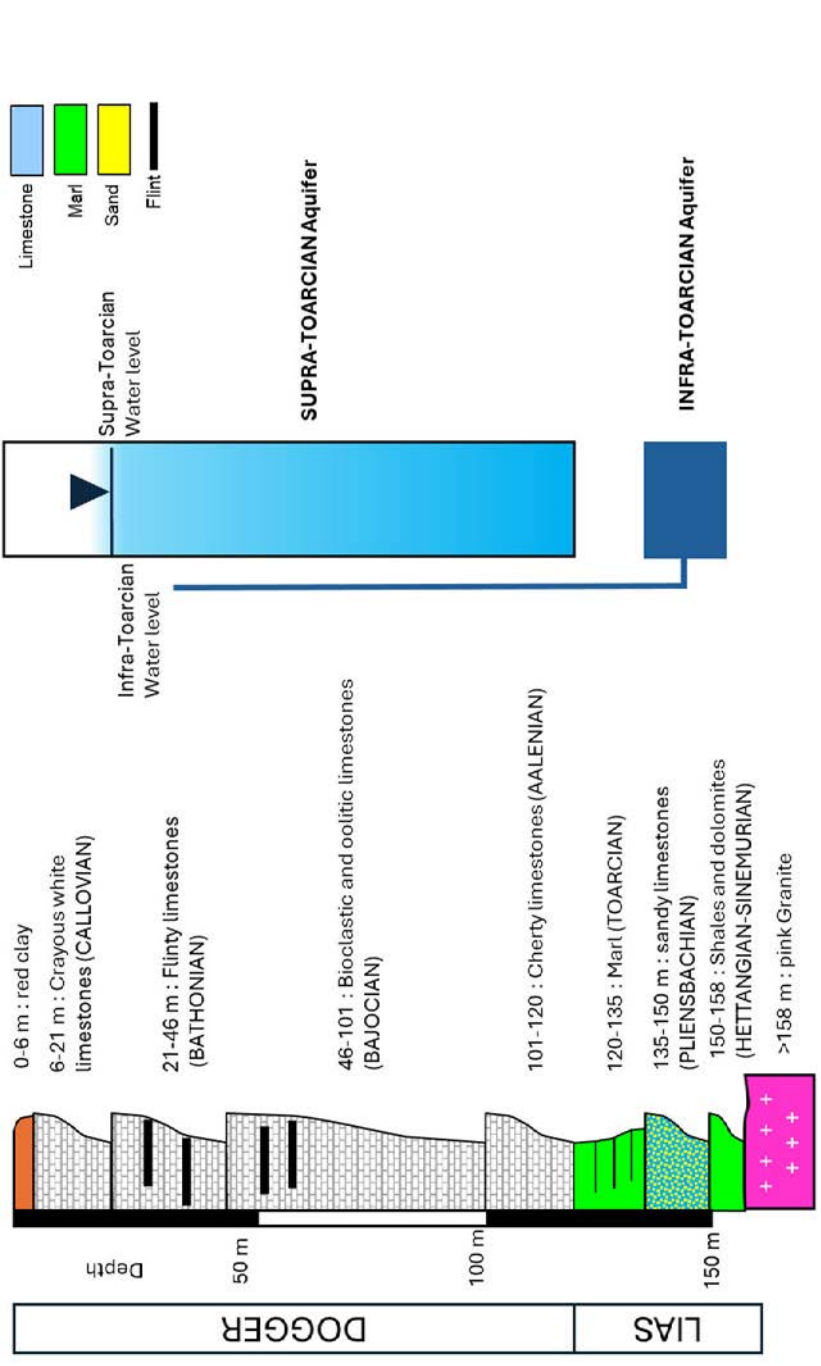


Figure 1 *Schematic cross-section of the Infra and Supra-Toarcian aquifers at the HES, Poitiers, France.*

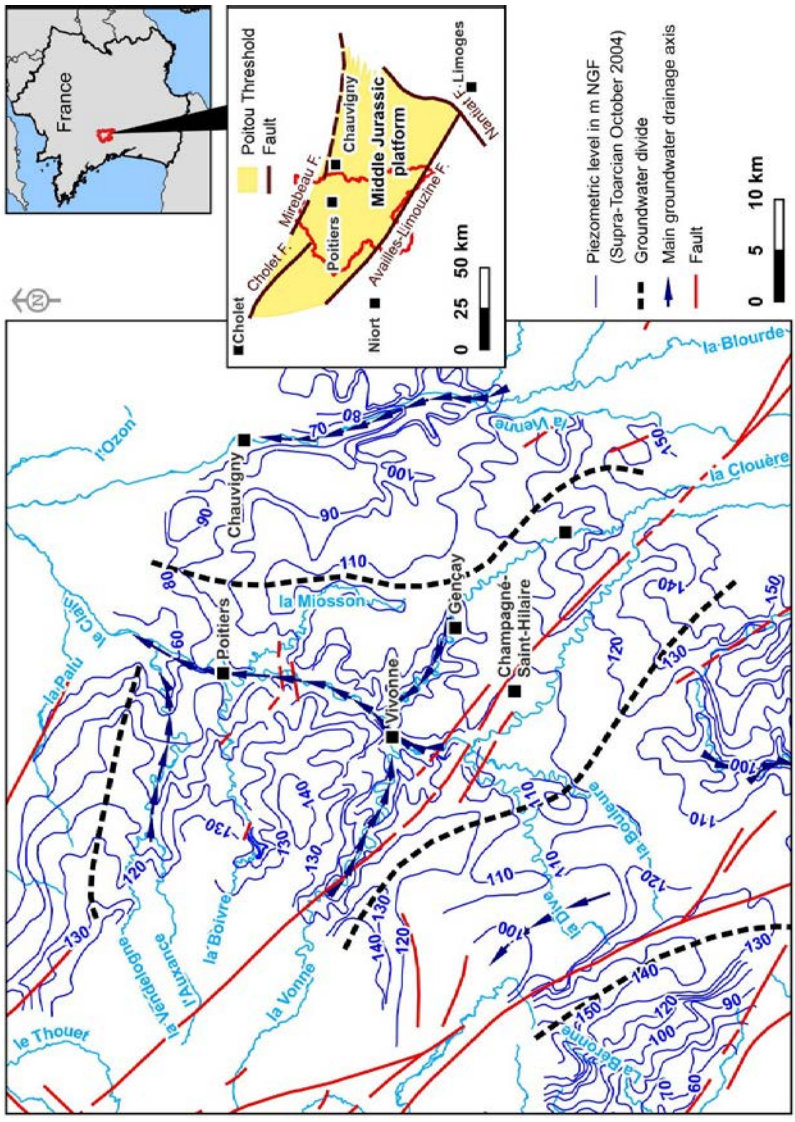


Figure 2 *Piezometric map of the supra-Toarcian aquifer (Marchais and Bichot, 2005, modified). mNGF: French elevation system above sea level in meters.*

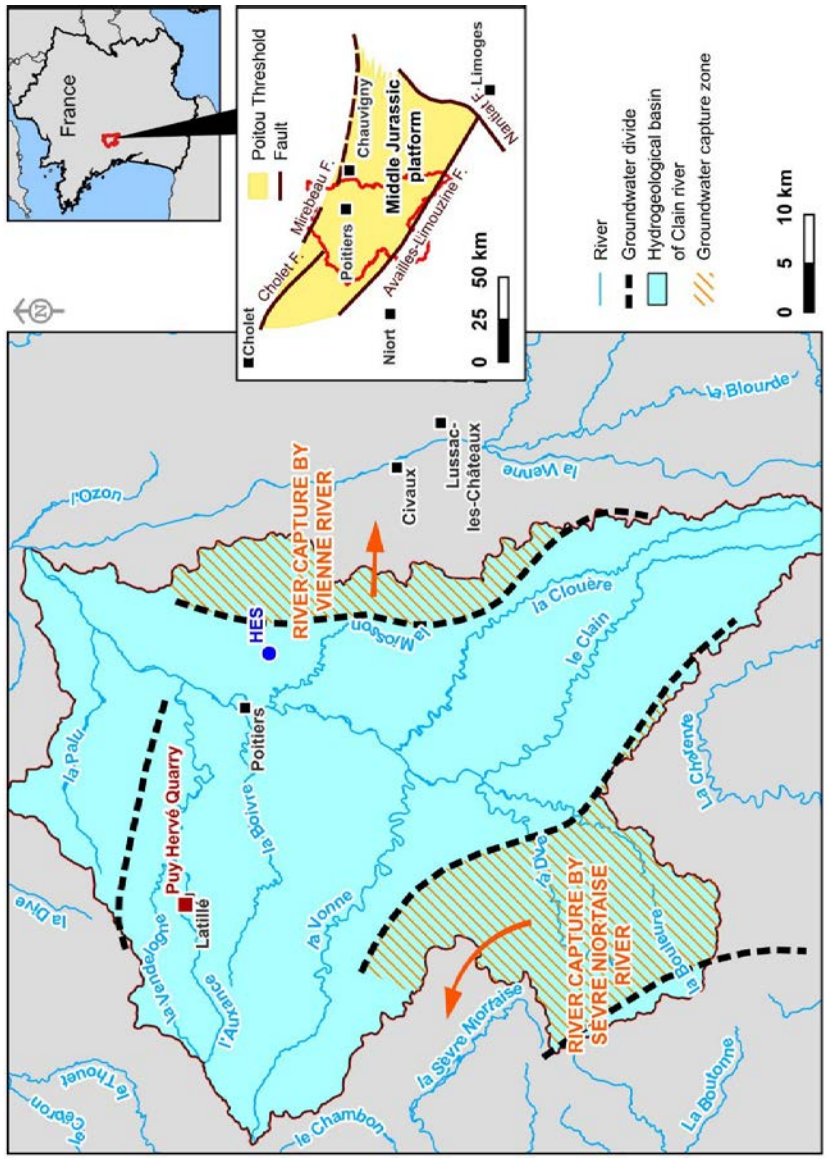


Figure 3 *Hydrogeological basin of Clain river.*

valley. Indeed, downcutting of the Vienne valley during the Mindel and Riss periods extended well beyond the paleovalleys of the Clain, which do not extend northward beyond Vivonne (46.42°N). The deeper incision of the Vienne valley into Supra-Toarcian formations south of Chauvigny enhances groundwater drainage toward the Vienne at the expense of the Clain basin. More recent, localized piezometric investigations have shown that this groundwater divide fluctuates spatially and temporally over several kilometers (Gaillard and Moreau, 2024). The piezometric map in Figure 3 depicts the easternmost position of the divide recorded to date. In the upstream part of the Clain watershed, another piezometric divide occurs south of the Availles-Limouzine Fault (Champagné-Saint-Hilaire Horst; see Gaillard, 2026). This divide separates the Clain from the Charente Basin, which drains westward to the Atlantic Ocean. Finally, to the southwestern part of the Clain Basin, a portion of groundwater is captured by the springs of the Sèvre Niortaise river via several karstic sinkholes located in the Dive-du-Sud valley. This karstic capture has been demonstrated by dye tracing experiments (Coirier, 1964).

# The supra-Toarcian aquifer

## *Groundwater flow patterns in the supra-Toarcian aquifer*

Groundwater flow in the Supra-Toarcian Aquifer exhibits characteristics of both a porous aquifer system—evidenced by piezometric mapping—and a karstic system, as demonstrated by numerous dye tracing tests and the exploration of karst networks by speleologists (Déribéré, 1937; SCP, 1990; Sibert et al., 2008).

The speleological networks explored within the Vienne département can be classified into two main types: introduction karsts and restitution karsts. Introduction karsts (also referred to as sinkholes or "gouffres") are circular depressions, sometimes reaching diameters of up to 100 m (e.g., the Gouffre du Grand Soubis in the Moulière Forest; Gouffre de la Troussaye at Marnay). Their depths generally do not exceed 50 m (e.g., 48 m at the Gouffre du Charreau de Boussec, Chauvigny). These features are predominantly vertical shafts, occasionally interrupted by ledges corresponding to bedding plane discontinuities. Restitution karsts are most commonly accessed through caves, and less frequently by cave diving. These systems include *laminoirs* (passages developed along bedding planes) and *trémies* (collapse zones connected to the surface). The galleries are typically sub-horizontal (Bigot, 2004, p. 105) and often display parallel orientations (SCP, 1990, p. 58).

As early as the 19th century, Longuemar (1856) highlighted the role of vertical fractures in controlling spring emergence at the contact with Toarcian marls. This model implicitly assumes that karst conduits develop preferentially along such fractures, supplied by concentrated recharge via sinkholes. Similarly, Welsch (1912) proposed a conceptual model in which dry valleys act as preferential drainage pathways toward springs. In this interpretation, decompression of the limestone massif within the dry valleys facilitates the karst conduit development. Official reports by hydrogeologists accredited by public health authorities consistently describe groundwater flow in these Jurassic limestones as occurring through fissure and conduit porosity, which locally generates preferential flow zones with high transmissivities (Mourrier et al., 1986).

## *Comparison between lineaments and speleological networks*

The dominant structural orientations in the study area include faults trending N115–125°, representing the main tectonic axis, and faults oriented N40–50°, corresponding to conjugate extension directions (Burbaud-Vergneaud, 1987). Additional orientations are also present, including N20–30°, N90°, N150°, and N180°.

To evaluate the influence of tectonics on the spatial organization of karst networks (restitution karst), a comparative analysis was carried out between lineament orientations and Speleological geometries in two study areas. The first area is centred on the largest known karst system of the Poitou Threshold (the Cuchon Cave system). The second encompasses the Hydrogeological Experimental Site (HES) of Poitiers University (Fig. 4). Lineaments were mapped by extracting elevation data from a 5 m resolution digital terrain model. Their orientations and lengths were used to construct stereo-net plots depicting the local tectonic framework. Karst void orientations for the Cuchon area were derived from a detailed speleological survey of the cave system (approximately 4 km of mapped passages). At the HES, fracture networks were characterized using the OPtical TeleViewer (OPTV) method, which produces high-resolution, magnetically oriented colour images of the borehole wall.

The results are shown in Figures 5 and 6. In the Cuchon area, the dominant lineament orientation is N45–55°E, whereas the surveyed karst conduits predominantly trend N130–140°E. This suggests that local fracturing does not exert primary control on the orientation of the Cuchon network galleries. At the HES, two regional fracture sets were identified, trending N50–65°E and N120–130°E. However, discontinuities observed in boreholes are mainly oriented between N80–100°E. These two examples indicate that restitution-type karst systems are only weakly influenced by regional fracturing patterns.


Figure 4 *Location of lineament analysis east of Poitiers (HES) and Chauvigny (Cuchon caves)*

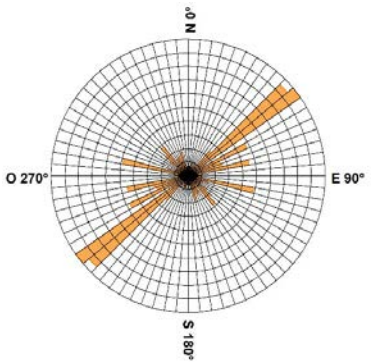


a) Lineaments

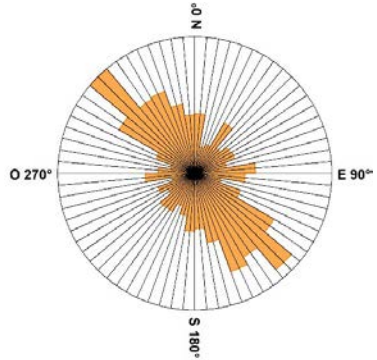


b) Cuchon network

Figure 5 *Comparison between lineament directions and the galleries direction of the Cuchon network caves*

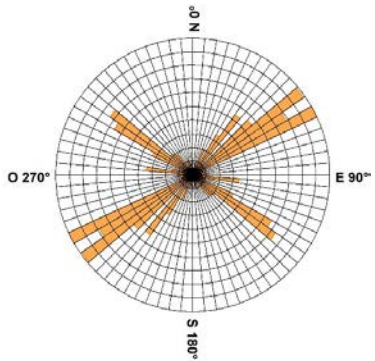


a) Lineaments

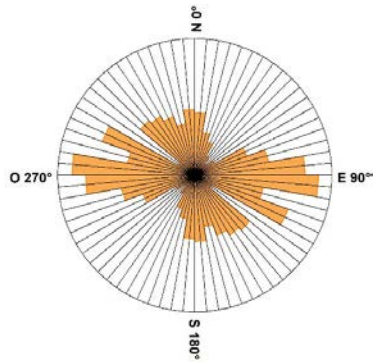


b) OPTV

Figure 6 *Comparison between lineament directions and OPTV direction in boreholes of HES.*

## *Typology of voids in Poitou threshold limestones*

For both study sites (HES and Cuchon Cave), the observed tectonic patterns do not coincide with the karst networks' orientations. This prompted an investigation into the potential role of stratigraphy in controlling karst development, based on analyses of primary cliff outcrops described in several doctoral dissertations on the Poitou Threshold (Benvel, 1978; Beaulieu, 1978; Balusseau, 1980; Mourrier, 1983). This work was presented during a field excursion of the French Chapter of the International Association of Hydrogeologists (www.cfh-aih.fr/colloques-et-visites/excursion-seuil-du-poitou-ag-12-au-15-03-2020.html and "Le karst du seuil du Poitou : Approche stratigraphique et rôle de la tectonique" on researchgate).

The methodology consisted of identifying macroporosity features in stratigraphically well-constrained outcrop sections. An illustrative example is shown in Figure 7, taken from the former Puy-Hervé quarry in Latillé, approximately 27 km west of Poitiers (see Fig. 3). Stratigraphic correlation was established through the collection of two index ammonite specimens: *Brasilia* sp. (Aalenian) and *Sonninia ovalis* (Early Bajocian). A distinct discontinuity separates the oolitic Aalenian formation from the gravelly limestones of the Bajocian. This surface, infilled with red clay, corresponds to Discontinuity D7 as defined by Gabilly et al. (1985). Locally, this discontinuity has been subject to dissolution, resulting in the development of macroporous zones within the limestone massif.

Using this method, two types of voids were identified, both in the examined outcrops and in the cores from the HES boreholes:

- type 1: scattered vacuoles within massive limestone beds, variably interconnected. These vacuolar levels are predominantly concentrated in the Lower Bajocian, specifically within the *Laeviuscula* and *Humphriesianum* ammonite zones;
- type 2: conduits aligned along stratigraphic discontinuities between two depositional sequences. These discontinuities are often filled with red clay, possibly corresponding to paleosol horizons. Their numbering follows the classification of Gabilly et al. (1985).

These void types are illustrated in Figure 8. They are not associated with vertical fractures. The dolomitization observed in certain formations was not considered in this analysis, as stratigraphic correlation was not possible due to the absence of paleontological markers in those units.

Type 1 voids are observed within the Bajocian limestones. In the area surrounding Poitiers (Boivre Valley, Clain Valley), these vacuoles are concentrated near the top of strata within the *Humphriesianum* zone and form distinct vuggy levels. Figure 9 shows an example from the Passelourdin cliff, located six kilometers south of Poitiers (Branger et al., 2026). In certain outcrops of Aalenian age (Gartempe Valley, east of Poitiers), calcite geodes of similar shape and size have been observed by the authors.

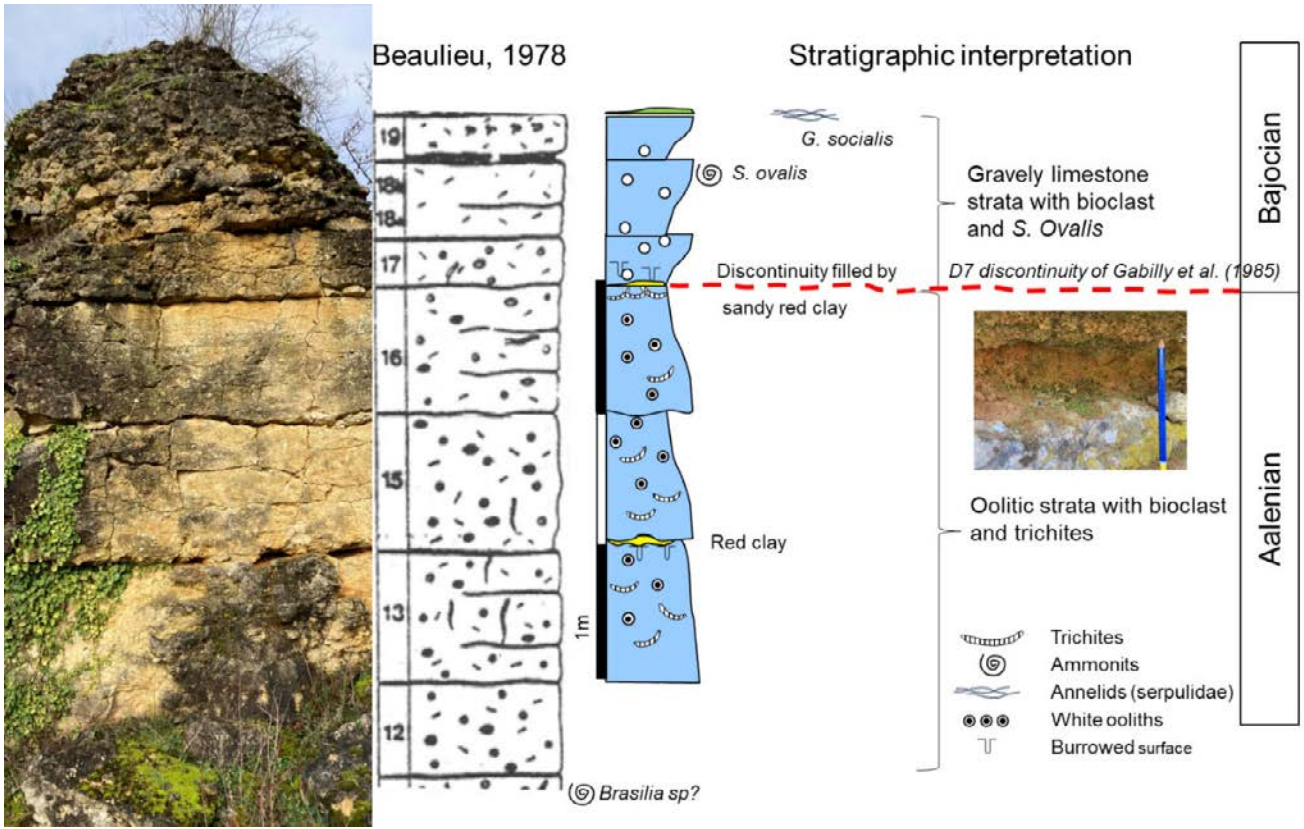


Figure 7 *Example of stratigraphical calibration of discontinuity in the supra-Toarcian aquifer (Latillé, Puy-Hervé quarry).*

a) Type 1 in Boivre Valley (Bajocian, *Humphriesianum* biozone)
Scale bar: 3 m

b) Type 1 in Clain valley (Bajocian, *Humphriesianum* biozone)

c) Type 2 at the bottom of Upper Bajocian (D8 discontinuity) at Poitiers

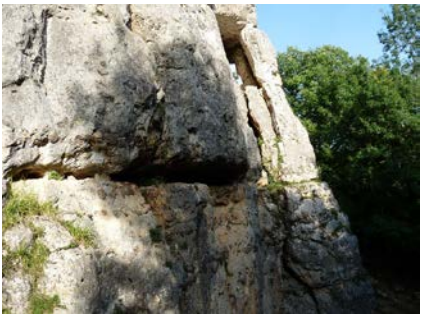

c) Type 2 at the top of the *Garantiana* biozone in the Bajocian (D8bis discontinuity)

Figure 8 *Typology of macroporosity in middle Jurassic limestones on Poitou Threshold.*

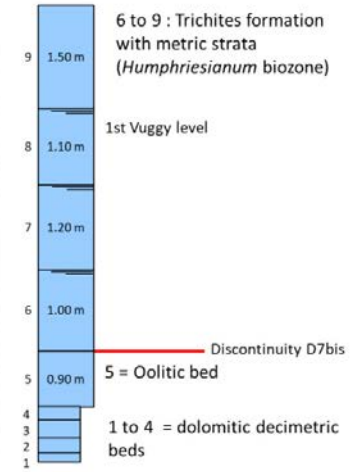


Figure 9 *Vuggy level in* Humphriesianum *zone of upper Bajocian (Saint Benoit - Passelourdin cliff).*

The spatial extent of Type 2 voids forms a sub-horizontal, interconnected macroporous system, due to the low dip of the strata. Locally, these voids form aligned conduits only a few centimeters in diameter, which may evolve into cave networks, such as those observed in Lussac-les-Châteaux, in the Vienne Valley (Fig. 10).


Figure 10 *Macroporosity on D8 discontinuity (Lussac-les-Châteaux cliff).*

## *Pumping tests*

On the Poitou Threshold, the Aalenian and Bajocian limestones are located within the saturated zone. These two geological formations are exploited for drinking water supply (19 million $m^3$/year according to SAGE Clain, 2011) and for agricultural irrigation (23 million $m^3$/year). Transmissivity values, estimated using the Cooper-Jacob method (1946), range from $10^{-2}$ to $10^{-3}$ $m^2/s$. The storage coefficient ranges between $10^{-2}$ and $10^{-4}$ depending on the borehole. These orders of magnitude were confirmed at the HES (Bernard, 2005). Two series of pumping tests were conducted in 2004 and 2005 after borehole drilling. Transmissivity values interpreted using the Cooper-Jacob method range from $2.2.10^{-3}$ to $4.4.10^{-3}$ $m^2/s$. Storage coefficients exhibit substantial variability over three orders of magnitude, ranging from $3.6.10^{-4}$ to $2.8.10^{-1}$. However, drawdown data cannot be consistently interpreted using a single straight line on a Cooper-Jacob semi-log plot, rendering the method ultimately inconclusive (Bernard, 2005, p. 125).

Three families of drawdown curves have been identified (Bernard, 2005): 1) The first exhibits a drawdown that doesn't follow a linear trend in the semi-log time domain; 2) The second displays two distinct linear segments in semi-log time, and 3) the third is characterized by a plateau or transition zone between two linear segments.

To improve curve fitting, a solution for interpreting interference pumping tests in a fractally fractured medium of Euclidean dimension two was developed using the

Cooper-Jacob equation (Delay et al., 2004). Bernard et al. (2008) demonstrated that permeability tends to homogenize rapidly over distances of 100–200 m, despite the drawdown data exhibiting significant variability and fractal characteristics. However, this fractal approach applied to fractures does not allow for calibration of the third family of curves. A different modelling approach has recently been applied to interpret pumping tests at the Civaux Nuclear Power Plant[1], located approximately 22 km southeast of Poitiers (see location on Fig. 3). This approach aims to account not only for fractures, but also for the influence of the porosity and permeability of the limestone blocks separating the horizontal discontinuities. The aquifer is conceptualized as containing regularly spaced horizontal discontinuities, which delimit rectangular limestone blocks of uniform thickness b (Fig. 11). For such an aquifer system, Streltsova (1976) proposed two drawdown equations: one for flow through fractures and another for flow through a porous matrix toward a pumping well operating at a constant discharge rate Q. The discontinuities are characterized by a hydraulic conductivity $K_f$ and specific storage Ssf, while the matrix possesses a hydraulic conductivity $K_m$ and specific storage Ssm.

To incorporate the flow dimensionality of Delay et al. (2004), the general Radial Flow equation of Barker was employed (Barker, 1988). This model generalized radial flow in an unsteady, n-dimensional, dual-porosity fractured aquifer. The flow dimension n governs the transition in flow behavior from linear to radial flow regimes. Exchange between the matrix and the fractures is controlled by a skin factor defined as $Sf = K_m b_s / (K_s b)$, where $b_s$ and $K_s$ denote respectively the thickness and hydraulic conductivity of the skin (the wall zone of the limestone block). Figure 11 illustrates pumping in a confined dual-porosity aquifer. The observed

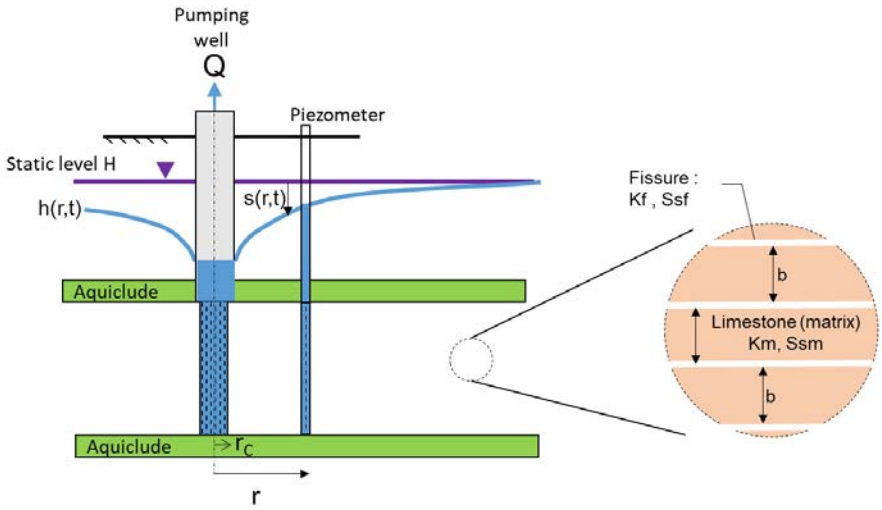


Figure 11 *Diagram illustrating cylindrical flow system (n=2) in a double porosity aquifer.*

1. © EDF 2024: these data are the property of EDF; any use is subject to EDF's prior agreement.

drawdown during a pumping test, at a distance r and time t, is denoted s(r,t) and reflects the total pressure change within the aquifer at the observation point, that is, the pressure variations in the fracture network.

Two examples of pumping tests are presented in Figure 12. On the left, graph (a) shows the results of a pumping test conducted at the HES. The drawdown was measured in observation well M2 during pumping at well M21 at a discharge rate of 62 $m^3/h$. Well M2 is located 103.7 meters from the pumping well. The drawdown derivative (ds) is shown in red and the drawdown curve in blue (HES) or green (Civaux). Initially, the derivative follows the trend of the drawdown, then decreases until approximately $10^4$ seconds. Thereafter, the derivative increases steadily until the end of the test. No wellbore storage disturbs the start of the drawdown curves. On the right, graph (b) presents the results of a pumping test conducted at Civaux[2]. The drawdown was measured at piezometer P1, located 37.2 meters from the pumping well P2. The discharge rate for this test was 51 $m^3/h$. The drawdown does not exhibit a linear relationship with the logarithm of time. The derivative appears to stabilize around $10^4$ seconds, then begins to increase again around $8.10^4$ seconds.

To compare the two pumping tests, graph (c) shows the drawdown derivatives of both tests using the dimensionless parameters defined by Streltsova (1976), namely $tD = Tt/(r^2S)$ and $sD = (2\pi s(r, t))/Q$, where t is the pumping time, r is the distance to the pumping well, T is the transmissivity, S is the storage coefficient, s(r,t) is the measured drawdown, and Q is the pumping rate. The transmissivity and storage coefficient values used were those obtained from fitting the early-time data to the Cooper-Jacob straight line. The two presented pumping tests also exhibit a similar dimensionless radius around $rD = 0.01$, allowing them to be compared on the same plot ($rD = r\sqrt{Km / K /b}$). Both pumping tests are plotted in graph (c) of Figure 12. The derivatives of both tests show very similar behaviour, structured in three distinct sequences[3]:

- early-time behavior: The derivative slope ranges between 0.4 and 0.7. This initial stage is interpreted as representing the flow contribution from the horizontal fracture network;
- intermediate-time behavior: The drawdown rate decreases, and the derivative stabilizes. This sequence is interpreted as the contribution from the rock matrix;
- late-time behavior: This phase reflects the combined influence of both fractures and matrix, where the pumping rate exceeds the crossflow from the matrix. As a result, drawdown does not stabilize but instead continues to increase over time.

This method was used to estimate aquifer parameters by interpreting eight pumping tests conducted at the HES and three tests at the Civaux site[4]. At the HES, for each test interpretation, two piezometers aligned with the pumping well were selected to analyse the drawdown curves. For both sites, the thickness of the matrix

2. © EDF 2024: these data are the property of EDF; any use is subject to EDF's prior agreement.
3. © EDF 2024: these data are the property of EDF; any use is subject to EDF's prior agreement
4. © EDF 2024: these data are the property of EDF; any use is subject to EDF's prior agreement

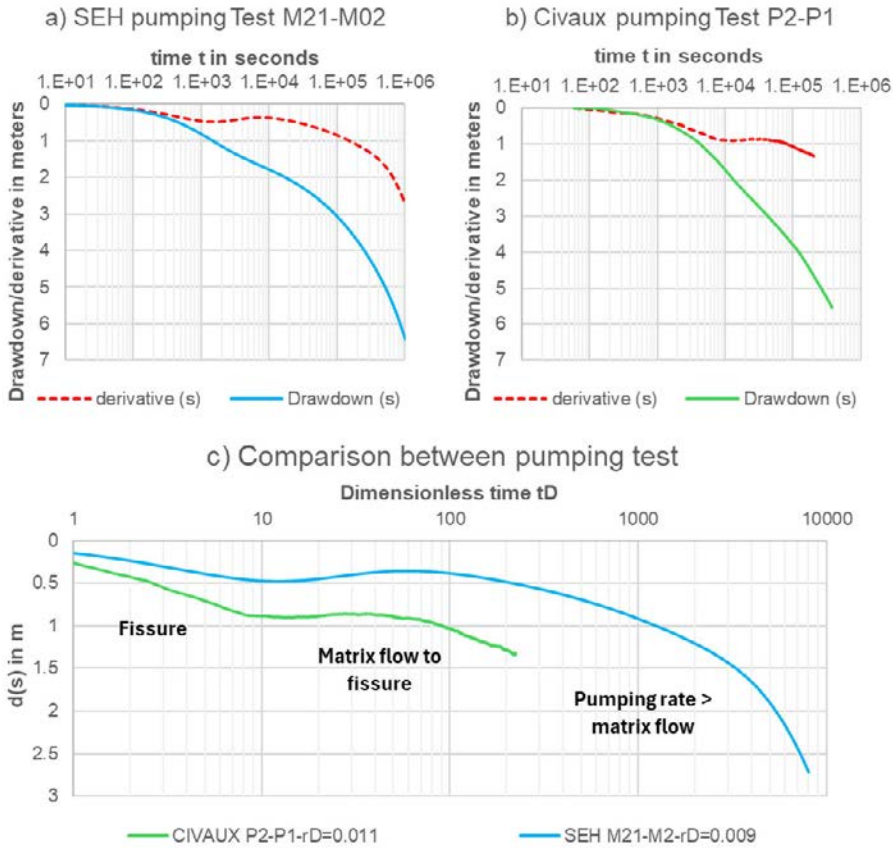


Figure 12 *Pumping test at constant rate. © EDF 2024: these data are the property of EDF; any use is subject to EDF's prior agreement.*

blocks was defined based on the stratigraphic interpretation of each borehole and on the identification of discontinuities between depositional sequences (Gaillard, 2026).

Figure 13 presents the results obtained from the pumping tests conducted at the HES site with AQTESOLV software. In the fracture medium, the hydraulic conductivity (K) appears to be homogeneous, with values ranging between $10^{-4}$ and $10^{-5}$ m/s. The specific storage (Ss) of the fractures varies between $10^{-6}$ and $10^{-3}$ $m^{-1}$. This parameter depends on fracture aperture and infilling material, which is consistent with field observations (Fig. 9 and 10) and borehole data. In contrast, data for the matrix are more scattered. The matrix hydraulic conductivity is several orders of magnitude lower than that of the fractures, with values ranging from $10^{-6}$ to $10^{-9}$ m/s. The specific storage of the matrix blocks appears to lie between $10^{-5}$ and $10^{-4}$ $m^{-1}$, with the highest value reaching $4.10^{-4}$ $m^{-1}$. The fracture skin factor (Sf) varies from 0 to 3, while the flow dimension (n) ranges between 1.5 and 2.

At Civaux (Fig. 14), the parameter values are less dispersed[5]. For the fracture network, hydraulic conductivity remains in the same order of magnitude ($10^{-4}$ to $10^{-5}$ m/s), and specific storage ranges from $10^{-5}$ to $10^{-4}$ $m^{-1}$. The results for the matrix are also within a narrow range: matrix hydraulic conductivity varies between $10^{-9}$ and $2.10^{-8}$ m/s, and the specific storage of the matrix blocks ranges from $10^{-5}$ to $10^{-4}$ $m^{-1}$.

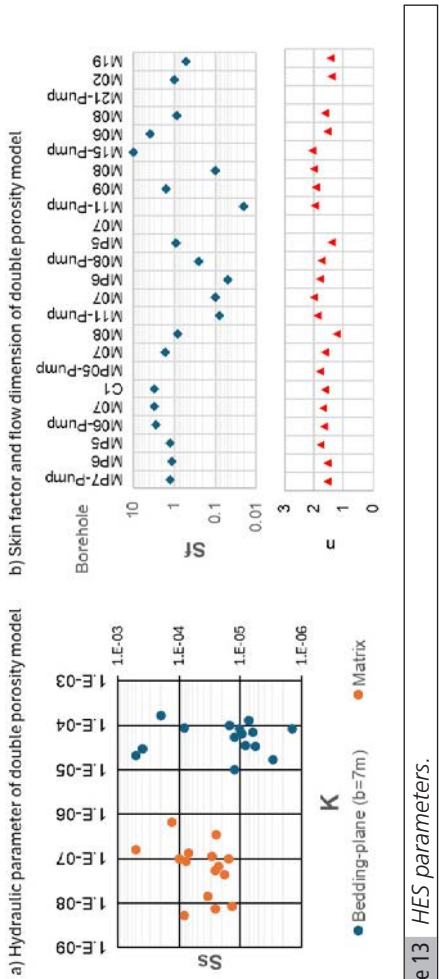


Figure 13 *HES parameters.*

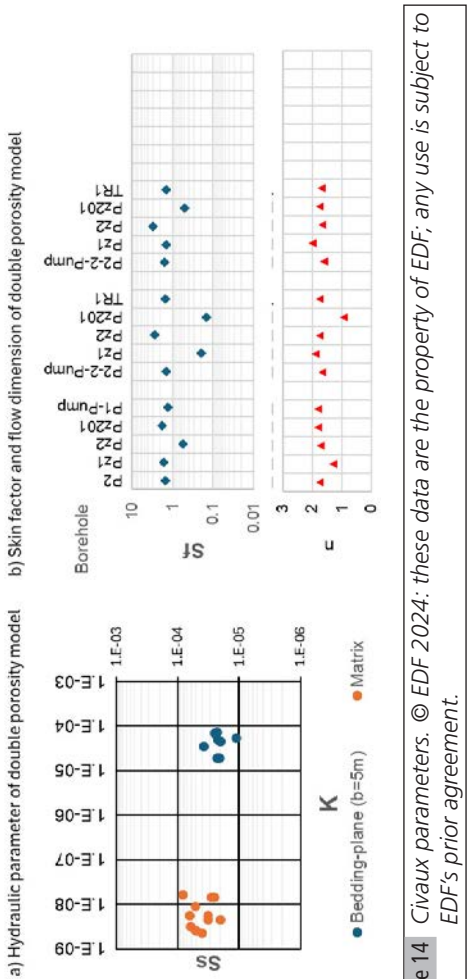


Figure 14 *Civaux parameters. © EDF 2024: these data are the property of EDF; any use is subject to EDF's prior agreement.*

5. © EDF 2024: these data are the property of EDF; any use is subject to EDF's prior agreement.

The dual-porosity model incorporating the flow dimension approach enables the calibration of all observed drawdown curves with a standard error less than 0.02. The matrix/discontinuity skin factor explains the various shapes observed in both the drawdown curves and their corresponding derivatives. An illustrative example is presented in Figure 15. The calibration was performed on both the drawdown curve and its derivative from a pumping test conducted at the HES. Graphs (a) show the drawdowns measured at observation well M19 during pumping at M21 (Q = 62.3 $m^3$/h). The test was calibrated using a skin factor value of Sf = 0. When the skin factor increases (Sf = 0.5 to 5), a plateau begins to appear on the drawdown

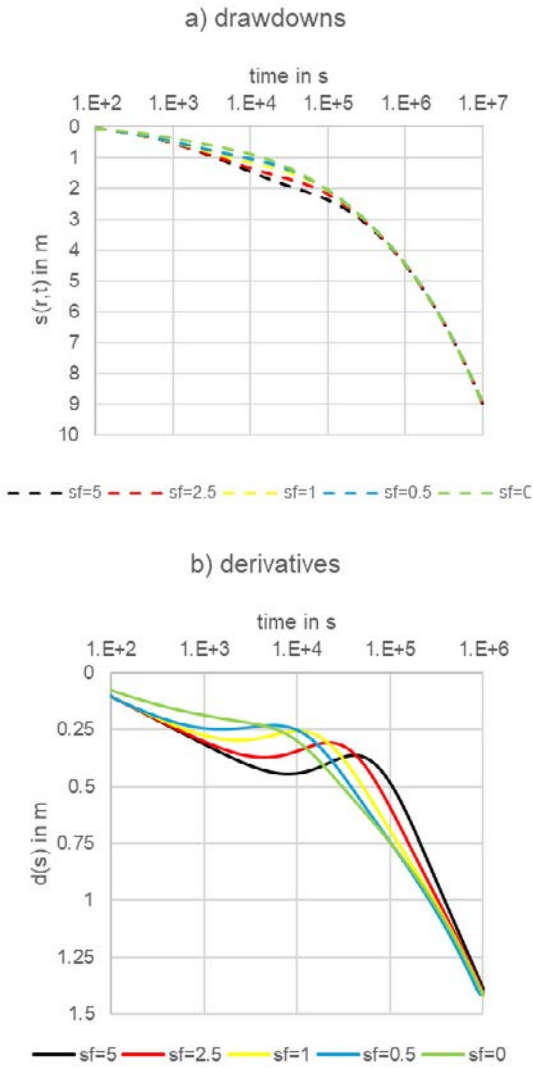


Figure 15 *Drawdown and derivative curves with and without Skin.*

curve. This phenomenon is even more evident in the drawdown derivatives shown in graph (b), where a wave-like shape forms in the derivative curve before dropping off.

Pumping test results from both the HES and the Civaux site[6] demonstrate that the heterogeneity of the supra-Toarcian aquifer can be effectively described using a dual-porosity conceptual model. This modelling approach is consistent with field data and highlights the role of sedimentary discontinuities in controlling groundwater flow.

## Conclusion

The Aalenian, Bajocian, and Bathonian limestones constitute microporous aquifers affected by various forms of karstic dissolution. Tectonic structures do not account for the location or geometry of speleological networks, the most extensive of which—the Cuchon Cave—reaches 4,000 m in mapped extent.

To explain the position of karstic outflow systems, a stratigraphic approach is required. Centimeter to decimeter-scale dissolution features have been correlated with the outcrop's stratigraphy. In non-dolomitized limestones, ovoid dissolution features are found within Lower Aalenian strata (*Opalinum* Zone) and Lower Bajocian strata (*Humphriesianum* Zone). Additional voids are associated with stratigraphic discontinuities separating sedimentary sequences. The regional extent of these discontinuities accounts for the recurrence of similar dissolution features in all valleys intersecting the Poitou Threshold.

Pumping tests conducted at two sites[7] on the threshold indicate that the Supra-Toarcian Aquifer behaves as a dual-porosity medium, with horizontal flow paths corresponding to bedding planes and discontinuities.

The role of stratigraphy is often underestimated in karst studies. Nevertheless, several works have demonstrated its importance in the development of horizontal karst systems (Esteban and Klappa, 1983) and in explaining intrinsic permeability variations in carbonate oil reservoirs (Reynolds, 1993). More recently, stratigraphic controls have been invoked to explain the distribution of macroporous levels in Upper Cretaceous Chalk formations in both Normandy (Gaillard et al., 2022) and England (Farrant et al., 2022). The stratigraphic correlation of karst features has revealed basin-scale trends in the Anglo-Norman Basin, enabling the prediction of karstic horizons. This approach is also applicable to the limestones of the supra-Toarcian aquifer of the Poitou Threshold.

6. © EDF 2024: these data are the property of EDF; any use is subject to EDF's prior agreement.
7. © EDF 2024: these data are the property of EDF; any use is subject to EDF's prior agreement

## Acknowledgements

The authors are grateful to thank Frédéric Lalbat (Electricité de France) for agreeing to use pumping tests at the Civaux site.

## References

Balusseau B. (1980). Le Jurassique inférieur et moyen sur la bordure nord-ouest du Limousin (région de Gouex à L'Isle-Jourdain, Vienne) [The Lower and Middle Jurassic on the north-western of the Limousin area (from Gouex to L'Isle-Jourdain, Vienne)]. Ph.D. thesis, University of Poitiers, France.

Barker J.A. (1988). A generalized radial flow model for hydraulic tests in fractured rock. *Water Resources Research*, 24(10): 1796-1804. https://doi.org/10.1029/WR024i010p01796

Beaulieu, G. (1978). Étude géologique des terrains jurassiques dans la région de Lusignan, Montreuil-Bonnin et Latillé: stratigraphie, cartographie et structure [Geological study of the Jurassic in the Lusignan, Montreuil-Bonnin and Latillé area : stratigraphy, cartography and structure]. Ph.D. thesis; University of Poitiers, France.

Bernard S. (2005). Caractérisation hydrodynamique des réservoirs carbonatés fracturés. Application au site expérimental hydrogéologique (SEH) de l'université de Poitiers [Hydrodynamic Characterization of Fractured Carbonate Reservoirs: Application to the Hydrogeological Experimental Site (HES) of the University of Poitiers]. Ph.D. thesis; University of Poitiers, France.

Bernard S., Delay F., Porel G. (2008). A new method of data inversion for the identification of fractal characteristics and homogenization scale from hydraulic pumping tests in fractured aquifers. *Journal of Hydrology*, 328(3-4): 647-658. https://doi.org/10.1016/j.jhydrol.2006.01.008

Benvel B. (1978). Étude stratigraphique, sédimentologique et structurale du Jurassique dans les vallées du Clain et de la Boivre en amont de Poitiers [Stratigraphic, sedimentological and structural study of the Jurassic in the Clain and Boivre valleys upstream of Poitiers]. Ph.D. thesis, University of Poitiers, France.

Bigot J.-Y. (2004). Spéléométrie de la France : Cavités classées par département, par dénivellation et développement, Situation au 31 décembre 2000 [Caving in France: Caves classified by department, by vertical drop and by development, Situation at December 31, 2000]. *Mémoire Spelunca* 27. https://spelunca-memoires.ffspeleo.fr/200407_Spelunca_memoires_27.pdf

Burbaud-Vergneaud M. 1987. Fracturation et interactions socle-couverture : le Seuil du Poitou [Fracturing and Basement-Cover Interaction: The Poitou Threshold]. Ph.D. thesis, University of Poitiers, France.

Branger P., Gailard T., Geairon H. (2026). "The stratigraphy of the Middle Jurassic of the Poitou threshold", Chapter 2 in *A new concept of karst development based on hydrogeology and geophysics*, EDP Sciences. https://doi.org/10.1051/978-2-7598-3934-6.c002

Coirier B. (1964). Essai de coloration à la fluorescéine des eaux de la Dive de Lezay, disparaissant au gouffre de « Jument blanche » près Bonneuil, commune de Sainte-Soline (Deux-Sèvres). Le problème de la source de la Sèvre Niortaise [Fluorescein dye tracer test of the Dive de Lezay, disappearing at the "Jument blanche" sinkhole near Bonneuil, commune of Sainte-Soline (Deux-Sèvres). The problem of the Sèvre Niortaise spring]. *Bulletin de l'Institut de Géologie et d'Anthropologie Préhistorique de la Faculté des Sciences de Poitiers*, V: 25-33.

Coirier B., Moreau P., Bourgueil B., Gabilly J. (1968). Hydrogéologie du plateau jurassique de Poitiers à Chauvigny [Hydrogeology of the Jurassic plateau from Poitiers to Chauvigny]. Bulletin de l'institut de Géologie et d'Anthropologie préhistorique, Université de Poitiers: 12-24.

Cooper H.H., Jacob C.E. (1946). A generalized graphical method for evaluating formation constants and summarizing well field history. *American Geophysical Union Transaction*, 27: 526-534. https://doi.org/10.1029/TR027i004p00526

Delay F., Porel G., Bernard S. (2004). Analytical 2D model to invert hydraulic pumping tests in fractured rocks with fractal behavior. Geophysical Research letters, Hydrology and Land Surface studies, 31(16). https://doi.org/10.1029/2004GL020500

Déribéré M. (1937). Les grottes de La Norée [La Norée caves]. *Spélunca*, 8: 19-23.

Esteban M., Klappa C. (1983). Subaerial exposure environments. In: P.A. Scholle, D.G. Bebout & C.H. Moore (Eds.): Carbonate depositional environments. American Association of Petroleum Geologists, Tulsa, 1-54.

Farrant A.R., Maurice L., Ballesteros D., Nehme C. (2022). The genesis and evolution of karstic conduit systems in the Chalk. Geological Society, London, Special Publications, 517. https://doi.org/10.1144/SP517-2020-126

Gaillard T., Branger P. (2026). "The Poitou Threshold", Chapter 1 in *A new concept of karst development based on hydrogeology and geophysics*, EDP Sciences. https://doi.org/10.1051/978-2-7598-3934-6.c001

Gaillard T. (2026). "Hydrostratigraphic study of the Hydrogeological Experimental Site of Poitiers, France", Chapter 8 in *A new concept of karst development based on hydrogeology and geophysics*, EDP Sciences. https://doi.org/10.1051/978-2-7598-3934-6.c008

Gabilly J., Cariou E., Hantzpergue P. (1985). Les grandes discontinuités du Jurassique : témoins d'évènements eustatiques, biologiques et sédimentaires [Major Jurassic discontinuities: evidence of eustatic, biological and sedimentary events]. *Bulletin de la Société Géologique de France*, I(3): 391-401. https://doi.org/10.2113/gssgfbull.I.3.391

Gaillard T., Hoyez B., Hauchard E. (2022). Contribution of stratigraphy to groundwater motion understanding in chalk: examples of karstogenic horizons of the Pointe de Caux, France. Geological Society of London, Special Publications, 517. https://doi.org/10.1144/SP517-2020-157

Gaillard T., Moreau M. (2024). Le Bajocien de la vallée du Miosson : Nouaillé-Maupertuis [Bajocian of Miosson valley : Nouaillé-Maupertuis]. In Le karst du seuil du Poitou : Approche stratigraphique et rôle de la tectonique, Livret Guide de l'excursion du CFH sur le seuil du Poitou, 29 au 31 mars 2024: 46-49.

Longuemar (Le Touzé de) A. (1856). Études sur la circulation naturelle des eaux superficielles et souterraines dans le département de la Vienne [Studies on the natural circulation of surface and ground water in the Vienne department]. Journal de la Vienne. Poitiers.

Marchais E., Bichot G. (2005). Référentiels piézométriques Phase 3 : Piézométries de l'aquifère du Dogger [Piezometric maps of the Dogger aquifer]. BRGM/RP-55847-FR.

Mourrier J.-P. (1983). Le versant parisien du seuil du Poitou de l'Hettangien au Bathonien. Stratigraphie, sédimentologie, caractères paléontologiques, Paleogéographie [The Parisian slope of the Poitou sill from the Hettangian to the Bathonian. Stratigraphy, sedimentology, paleontological features, paleogeography]. Ph.D. thesis, University of Poitiers, France.

Mourier J.-P., Gabilly J., Platel J.-P. (1986). Carte géologique de la France : Notice explicative de la feuille Poitiers à 1/50000 [Geological map of France: note for the Poitiers 1:50,000 sheet]. BRGM.

Reynolds A.D. (1993). Sedimentology and sequence stratigraphy of the Thistle field, northern North Sea, In Sequence Stratigraphy on the Northwest European Margin by Steel R.J., Felt V.L., Johannesson E.P., Mathieu C. (Editors). *Norwegian Petroleum Society Special Publications*, 5: 257-271.

Schéma d'Aménagement et de Gestion des Eaux du Clain "SAGE" (2011). État Initial (water development and management scheme for the river Clain (SAGE), 2011. initial status).

Sibert E., Loiseau C., Rouy J.-L. (2008). La grotte de la Vallée Cuchon (Chauvigny, Vienne) [Cuchon valley cave, Chauvigny, Vienne]. *Spelunca*, 10: 21-26.

SCP/ Spéléo-Club Poitevin (1990). Bilan d'activités.

Streltsova T.D. (1976). Hydrodynamics of groundwater flow in a fractured formation. Water Resources Research, 12(3): 405-414. https://doi.org/10.1029/WR012i003p00405

Welsch J. (1912). Hydrologie souterraine du Poitou calcaire [Underground hydrology of the Poitou limestone area]. Spelunca, IX (69).